# Rate-Determining Factors in Nucleophilic Aromatic Substitution Reactions

Israel Fernández,[†] Gernot Frenking,[‡] and Einar Uggerud*,[§]

[†]*Departamento de Química Orgánica, Facultad de Química, Universidad Complutense, 28040-Madrid, Spain,* [‡]*Fachbereich Chemie, Philipps-Universität Marburg, Hans-Meerwein-Strasse, D-35043 Marburg, Germany, and* [§]*Massespektrometrilaboratoriet og Senter for teoretisk og beregningsbasert kjemi (CTCC), Kjemisk institutt, Universitetet i Oslo, Postboks 1033 Blindern, N-0315 Oslo, Norway*

einar.uggerud@kjemi.uio.no

Received February 11, 2010
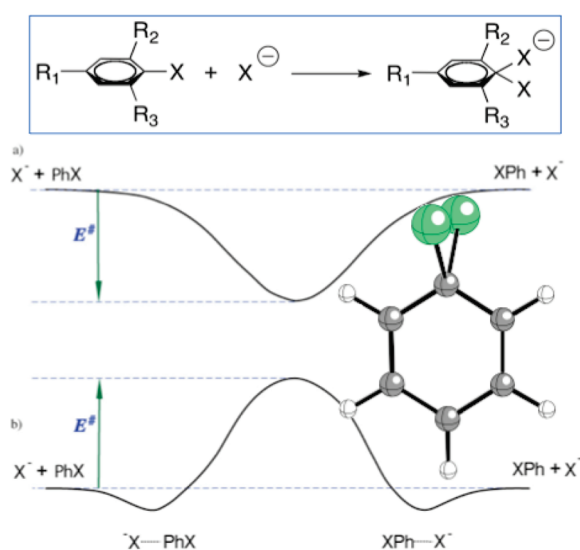
S_NAr: Minimum or TS?

Quantum chemical calculations (OPBE/6-311++G(d,p)) have been performed to uncover the electronic factors that govern reactivity in the prototypical S_NAr reaction. It was found that intrinsic nucleophilicity—expressed as the critical energy (the energy required for forming the Meisenheimer structure $Ph(X)_2^-$) in the identity substitution reaction $X^- + PhX \rightarrow X^- + PhX$ (Ph = phenyl)—shows the following approximate trend: $NH_2^- \approx OH^- \approx F^- \gg PH_2^- \approx SH^- \approx Cl^- > AsH_2^- \approx SeH^- \approx Br^-$. The periodic trends are discussed in terms of molecular properties (proton affinity of X^- expressing Lewis basicity of the nucleophile and C(1s) orbital energy expressing Lewis acidity of the substrate) based on a dative bonding model. Furthermore, the stepwise progress of the reactions and the critical structures are analyzed applying energy decomposition analysis. Increased stability, and thereby increased intrinsic nucleophilicity, correlates with decreasing aromatic character of the Meisenheimer structure. This apparent contradiction is explained in consistency with the other observations using the same model.

Introduction

Nucleophilic aromatic substitution reactions are of considerable practical use for transformations in medicinal and agricultural chemistry, facilitating, for example, the introduction of fluorine to aromatic skeletons useful for application in, for example, positron emission tomography (PET).[1−3] Besides widespread relevance to organic chemistry, the reaction type is

(1) Smith, M. B.; March, J. *March's Advanced Organic Chemistry: Reactions, Mechanisms, and Structure*, 6th ed.; John Wiley: New York, 2007.

(2) Chambers, R. D. *Fluorine in Organic Chemistry*; Blackwell: Oxford, 2004.
(3) Terrier, F. *Chem. Rev.* **1982**, *82*, 78.
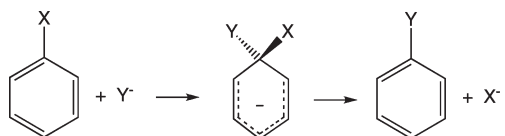
also encountered in biological dechlorination reactions, for which gluathinone transferase[4] and 4-chlorobenzoyl-coenzyme A dehalogenase[5] are examples of key enzymes operating according to this mode of reactivity. Nucleophilic aromatic substitution may occur according to several different mechanistic schemes, of which the S_NAr mechanism is the most important.[6−8] The typical S_NAr reaction is characterized by the simple two-step addition/elimination mechanism illustrated in Scheme 1, in which the intermediate Meisenheimer σ adduct, first isolated in the form of a salt in 1902, is central. Reactions of the S_NAr type have also been investigated in the isolated gas phase, both experimentally[9−19] (Kebarle, Cooks, Danikiewicz) and computationally,[18,20−24] and the results of the gas-phase studies confirm the general mechanistic picture based on observations in the condensed phases. At first sight, the existence of stable Meisenheimer adducts may appear counterintuitive since they represent situations where ring aromaticity is broken by the introduction of extra electron density. However, one needs to take into account the fact that the stability of a Meisenheimer adduct is usually obtained by substituting electron-withdrawing groups to the aromatic ring. On the other hand, little activation of this type appears to be necessary to accommodate the reaction since the rather weak electron deficiencies in the aromatic ring of nitrobenzene and in particular fluorobenzene allow for displacement of nitrite and fluoride, respectively, by fluoride.[18,22] Besides the obvious aspect of activation by electron-withdrawing groups, relatively little systematic knowledge of other factors that influence reactivity is known. Of these factors, the properties of the nucleophile/nucleofuge (incoming/leaving group) pair are of particular interest.

To our knowledge, only one paper has addressed this question in a systematic fashion, and then only partly so. On the basis of quantum chemical calculations, Glukhovtsev et al.[22] demonstrated that for the identity reaction $C_6H_5X + X^- \rightarrow C_6H_5X + X^-$ (X = halide), only fluoride gives rise to a stable Meisenheimer adduct.

For the cases of chloride, bromide, and iodine, Glukhovtsev et al. found that the symmetrical Meisenheimer adduct is not stable in the sense that it both has higher energy than the separated reactants $PhX + X^-$ as well as represents a transition structure and not a potential energy minimum. However, Gluhkovtsev et al. did not investigate nucleophiles/nucleofuges other than the halides.

We have previously addressed aliphatic S_N2 reactivity in a systematic fashion in a series of papers,[25−29] establishing and applying various quantum chemical methodologies for analyzing reactivity in terms of critical energy factors. The outcome of these studies has been manifold: demonstrating and explaining reactivity trends in terms of physical observables, relating these to periodic table order, demonstrating strong solvent effects, and clarifying physical organic chemistry terms like nucleophilicity and steric effect. In the present paper, we will apply this type of analysis to nucleophilic aromatic substitution reactions, the S_NAr reaction, and at the same time extend the knowledge to nucleophiles other than the halides.

In a typical aliphatic S_N2 reaction, the symmetrical trigonal bipyramidal geometric arrangement with the nucleophile and nucleofuge in the axial positions corresponds to a saddle point of the potential energy surface, equivalent to a transition structure. However, in some cases, dependent on the chemical nature of nucleophile and substrate, the same geometric arrangements is instead found to give a minimum energy structure.[30−35] In this respect, there are obvious similarities between S_N2 and S_NAr. It would be of great interest to know how this topographic variability is related to the underlying electronic structures. In other words, we need to know if nucleophilicity is a universal property[36] or if there only exists separate aliphatic and aromatic nucleophilicities.

Methods

Molecular geometries were optimized using DFT theory applying the OPBE functional.[37,38] This choice of method is partly dictated by the fact that it has been demonstrated to provide good accuracy in reproducing important physical

(4) Zheng, Y.-J.; Ornstein, R. L. *J. Am. Chem. Soc.* **1997**, *119*, 648.

(5) Xu, D.; Wei, Y.; Wu, J.; Dunaway-Mariano, D.; Guo, H.; Cui, Q.; Gao, J. *J. Am. Chem. Soc.* **2004**, *126*, 13649.

(6) Bunnett, J. F.; Zahler, R. E. *Chem. Rev.* **1951**, *49*, 273.

(7) Ingold, C. K. *Structure and Mechanism in Organic Chemistry*; Cornell University Press: Ithaca, NY, 1953.

(8) Bernasconi, C. F. *Chimia* **1980**, *31*, 1.

(9) Briscese, S. M. J.; Riveros, J. M. *J. Am. Chem. Soc.* **1975**, *97*, 230.

(10) Dzidic, I.; Carroll, D. I.; Stillwell, R. N.; Horning, E. C. *Anal. Chem.* **1975**, *47*, 1308.

(11) Bowie, J. H.; Stapleton, B. J. *Aust. J. Chem.* **1977**, *30*, 795.

(12) Kleingeld, J. C.; Nibbering, N. M. M. *Tetrahedron Lett.* **1980**, *21*, 1687.

(13) Ingemann, S.; Nibbering, N. M. M.; Sullivan, S. A.; DePuy, C. H. *J. Am. Chem. Soc.* **1982**, *104*, 6520.

(14) Hiraoka, K.; Mizuse, S.; Yamabe, S. *J. Phys. Chem.* **1987**, *91*, 5294.

(15) Dillow, G. W.; Kebarle, P. *J. Am. Chem. Soc.* **1988**, *110*, 4877.

(16) Danikiewicz, W.; Bienkowski, T.; Poddebniak, D. *J. Am. Soc. Mass. Spectrom.* **2004**, *15*, 927.

(17) Chen, H.; Chen, H.; Cooks, R. G. *J. Am. Soc. Mass. Spectrom.* **2004**, *15*, 998.

(18) Giroldo, T.; Xavier, L. A.; Riveros, J. M. *Angew. Chem., Int. Ed.* **2004**, *43*, 3588.

(19) Chiavarino, B.; Crestoni, M. E.; Fornarini, S.; Lanucara, F.; Lemaire, J.; Maítre, P. *Angew. Chem., Int. Ed.* **2007**, *46*, 1995.

(20) Simkin, B. Y.; Gluz, E. B.; Glukhovtsev, M. N.; Minkin, V. I. *THEOCHEM* **1993**, *284*, 123.

(21) Buncel, E.; Tarkka, R. M.; Dust, J. M. *Can. J. Chem.* **1994**, *72*, 1709.

(22) Glukhovtsev, M. N.; Bach, R. D.; Laiter, S. *J. Org. Chem.* **1997**, *62*, 4036.

(23) Haoran, S.; Stephen, G. D. *Angew. Chem., Int. Ed.* **2006**, *45*, 2720.

(24) Pliego, J. R.; Pilo-Veloso, D. *Phys. Chem. Chem. Phys.* **2008**, *10*, 1118.

(25) Laerdahl, J. K.; Civcir, P. U.; Bache-Andreassen, L.; Uggerud*, E. *Org. Biomol. Chem.* **2006**, *4*, 135.

(26) Uggerud, E. *Chem.—Eur. J.* **2006**, *12*, 1127.

(27) Ochran, R. A.; Uggerud, E. *Int. J. Mass spectrom.* **2007**, *265*, 169.

(28) Fernández, I.; Frenking, G.; Uggerud, E. *Chem.—Eur. J.* **2009**, *15*, 2166.

(29) Uggerud, E. *Pure Appl. Chem.* **2009**, *81*, 709.

(30) Solling, T. I.; Pross, A.; Radoma, L. *Int. J. Mass Spectrom.* **2001**, *210/211*, 1.

(31) Solling, T. I.; Radom, L. *Chem.—Eur. J.* **2001**, *7*, 1516.

(32) Solling, T. I.; Radom, L. *Eur. J. Mass Spectrom.* **2000**, *6*, 153.

(33) Solling, T. I.; Wild, S. B.; Radom, L. *Inorg. Chem.* **1999**, *38*, 6049.

(34) vanBochove, M. A.; Swart, M.; Bickelhaupt, F. M. *J. Am. Chem. Soc.* **2006**, *128*, 10738.

(35) Pierrefixe, S. C. A. H.; Guerra, C. F.; Bickelhaupt, F. M. *Chem.—Eur. J.* **2008**, *14*, 819.

(36) Phan, T. B.; Breugst, M.; Mayr, H. *Angew. Chem., Int. Ed.* **2006**, *45*, 3869.

(37) Handy, N. C.; Cohen, A. J. *Mol. Phys.* **2001**, *99*, 403.

(38) Perdew, J. P.; Burke, K.; Ernzerhof, M. *Phys. Rev. Lett.* **1996**, *77*, 3865.

parameters including reaction barriers[39,40] and partly because we used it for our previous analysis of S_N2 reaction energetics.[28] The basis set used, 6-311++G(d,p), has triple-ζ quality augmented by two sets of polarization functions and two diffuse functions. This level of theory is denoted OPBE/6-311++G-(d,p). Vibrational frequencies of all optimized structures were calculated to inspect the nature of the stationary points (minimum or transition structure). The calculations were carried out with the GAUSSIAN 03 suite of programs.[41]

The interactions were analyzed by means of the scheme for energy decomposition analysis (EDA) inherent in the ADF program package.[42] This scheme was developed by Ziegler and Rauk[43] which was based on a similar procedure proposed by Morokuma.[44] Briefly explained, the scheme is set up for analyzing the interaction between two fragments in terms of an instantaneous interaction energy, ΔE_{int} defined to be the energy difference between the supermolecule describing the system of interest and the separated fragments in the same geometric arrangement of atoms they have in the supermolecule and in the proper electronic reference state. The interaction energy can be divided into three main components:

$$\Delta E_{int} = \Delta E_{elstat} + \Delta E_{Pauli} + \Delta E_{orb} \quad (I)$$

ΔE_{elstat} gives the electrostatic interaction energy between the fragments, which are calculated using the frozen electron density distribution of the fragments in the geometry of the supermolecule. The second term in eq I, ΔE_{Pauli}, refers to the repulsive interactions between the fragments, which are caused by the fact that two electrons with the same spin cannot occupy the same region in space. ΔE_{Pauli} is calculated by enforcing the Kohn–Sham determinant on the superimposed fragments to obey the Pauli principle by antisymmetrization and renormalization. The stabilizing orbital interaction term, ΔE_{orb}, is calculated in the final step of the energy partitioning analysis when the Kohn–Sham orbitals relax to their optimal form. This term can be further partitioned into contributions by the orbitals belonging to different irreducible representations of the point group of the interacting system. The interaction energy, ΔE_{int}, can be used to calculate the bond dissociation energy, D_e, by adding ΔE_{prep}, which is the energy necessary to promote the fragments from their equilibrium geometry to the geometry in the supermolecule (eq II). The advantage of using ΔE_{int} instead of D_e is that the instantaneous electronic interaction of the fragments becomes analyzed which yields a direct estimate of the energy components. Further details about the EDA can be found in the literature.[45–50]

$$-D_e = \Delta E_{prep} + \Delta E_{int} \quad (II)$$

As a geometric criterion for aromaticity, we have used the harmonic oscillator model of aromaticity (HOMA).[51,52] The evaluation of the HOMA values for the six-membered rings was carried out according to the following equation

$$HOMA = 1 - \frac{1}{N}\alpha_{CC}\sum_{i=1}^{N}(R_{CC}^{opt} - R_{CC}^i)^2 \quad (III)$$

where N is the number of bonds taken into the summation (in our case, six); α_{CC} is an empirical constant fixed to give HOMA = 0 for a model nonaromatic system, and HOMA = 1 for a system, like the benzene molecule, with all bonds equal to an optimal value R^{opt}, assumed to be realized for fully aromatic systems. R^i are actual bond lengths.

As a magnetic criterion for aromaticity, we have used the anisotropy of the induced current density (AICD) method[53,54] applying the continuous set of gauge transformation (CSGT) method of Keith and Bader[55–57] to calculate the current densities at the OPBE/6-311++G(d,p) level.

Results and Discussion

To simplify our discussion about factors that govern reactivity, we will here only consider the energy demands of identity reactions. It is well known that the effect of exothermicity on nonidentity substitutions, where one group, X, is replaced by another, Y, may be considerable, and for strongly exothermic reactions it may even become the dominating factor. However, the relative importance of the thermodynamic driving force on the one hand and the intrinsic barrier in determining the critical energy (barrier height, energy of activation), on the other hand, can be estimated with good accuracy by applying a Hammond- or Marcus-type formalism.[58,59] Within this formalism, the intrinsic reactivity of each nucleophile/nucleofuge is obtained from the corresponding identity reaction. From this point of view, the critical energy of an identity nucleophilic substitution reaction defines the intrinsic nucleophilicity of that particular X group. For identity reactions, we envisage two different potential energy functions depending on whether the symmetrical Meisenheimer-type corresponds to a minimum or a transition structure (Figure 1a and b). The typical gas-phase S_NAr reaction is characterized by the single-well potential energy function illustrated in Figure 1a,

(39) Swart, M.; Ehlers, A. W.; Lammertsma, K. *Mol. Phys.* **2004**, *102*, 2467.
(40) Swart, M.; Sol, M.; Bickelhaupt, F. M. *J. Comput. Chem.* **2007**, *28*, 1551.
(41) Frisch, M. J.; Trucks, G. W.; Schlegel, H. B.; Scuseria, G. E.; Robb, M. A.; Cheeseman, J. R.; Montgomery, J. A., Jr.; Vreven, T.; Kudin, K. N.; Burant, J. C.; Millam, J. M.; Iyengar, S. S.; Tomasi, J.; Barone, V.; Mennucci, B.; Cossi, M.; Scalmani, G.; Rega, N.; Petersson, G. A.; Nakatsuji, H.; Hada, M.; Ehara, M.; Toyota, K.; Fukuda, R.; Hasegawa, J.; Ishida, M.; Nakajima, T.; Honda, Y.; Kitao, O.; Nakai, H.; Klene, M.; Li, X.; Knox, J. E.; Hratchian, H. P.; Cross, J. B.; Bakken, V.; Adamo, C.; Jaramillo, J.; Gomperts, R.; Stratmann, R. E.; Yazyev, O.; Austin, A. J.; Cammi, R.; Pomelli, C.; Ochterski, J. W.; Ayala, P. Y.; Morokuma, K.; Voth, G. A.; Salvador, P.; Dannenberg, J. J.; Zakrzewski, V. G.; Dapprich, S.; Daniels, A. D.; Strain, M. C.; Farkas, O.; Malick, D. K.; Rabuck, A. D.; Raghavachari, K.; Foresman, J. B.; Ortiz, J. V.; Cui, Q.; Baboul, A. G.; Clifford, S.; Cioslowski, J.; Stefanov, B. B.; Liu, G.; Liashenko, A.; Piskorz, P.; Komaromi, I.; Martin, R. L.; Fox, D. J.; Keith, T.; Al-Laham, M. A.; Peng, C. Y.; Nanayakkara, A.; Challacombe, M.; Gill, P. M. W.; Johnson, B.; Chen, W.; Wong, M. W.; Gonzalez, C.; Pople, J. A. Gaussian, Inc.: Wallingford, CT, 2004.
(42) Baerends, E. J. e. a. Scientific Computing & Modelling NV: Amsterdam, The Netherlands, 2007.
(43) Ziegler, T.; Rauk, A. *Theor. Chim. Acta* **1977**, *46*, 1.
(44) Morokuma, K. *J. Chem. Phys.* **1971**, *55*, 1236.
(45) Lein, M.; Frenking, G. In *Theory and Applications of Computational Chemistry: The First 40 Years*; Dykstra, C. E., Frenking, G., Kim, K. S., Scuseria, G. E., Eds.; Elsevier: Amsterdam, 2005, p 291.

(46) *Reviews In Computational Chemistry*; Bickelhaupt, F. M., Baerends, E. J., Eds.; Wiley-VCH, Inc.: New York, 2000; Vol. 15.
(47) Velde, G. T.; Bickelhaupt, F. M.; Baerends, E. C.; Guerra, C. F.; Gisbergen, S. J. A. V.; Snijders, J.; Ziegler, T. *J. Comput. Chem.* **2001**, *22*, 931.
(48) Frenking, G.; Wichmann, K.; Fröhlich, N.; Loschen, C.; Lein, M.; Frunzke, J.; Rayón, J. M. *Coord. Chem. Rev.* **2003**, *238–239*, 55.
(49) Krapp, A.; Bickelhaupt, F. M.; Frenking, G. *Chem.—Eur. J.* **2006**, *12*, 9196.
(50) Esterhuysen, C.; Frenking., G. *Theor. Chem. Acc.* **2004**, *111*, 381.
(51) Krygowski, T. M. *J. Chem. Inf. Comp. Sci.* **1993**, *33*, 70.
(52) Cyranski, M. K. *Chem. Rev.* **2005**, *105*, 3773.
(53) Herges, R.; Geuenich, D. *J. Phys. Chem. A* **2001**, *105*, 3214.
(54) Geuenich, D.; Hess, K.; Kohler, F.; Herges, R. *Chem. Rev.* **2005**, *105*, 3758.
(55) Keith, T. A.; Bader, R. F. W. *Chem. Phys. Lett.* **1992**, *194*, 1.
(56) Keith, T. A.; Bader, R. F. W. *J. Chem. Phys.* **1993**, *99*, 3669.
(57) Cheeseman, J. R.; Trucks, G. W.; Keith, T. A.; Frisch, M. J. *J. Chem. Phys.* **1996**, *104*, 5497.
(58) Wolfe, S.; Mitchell, D. J.; Schlegel, H. B. *J. Am. Chem. Soc.* **1981**, *103*, 7694.
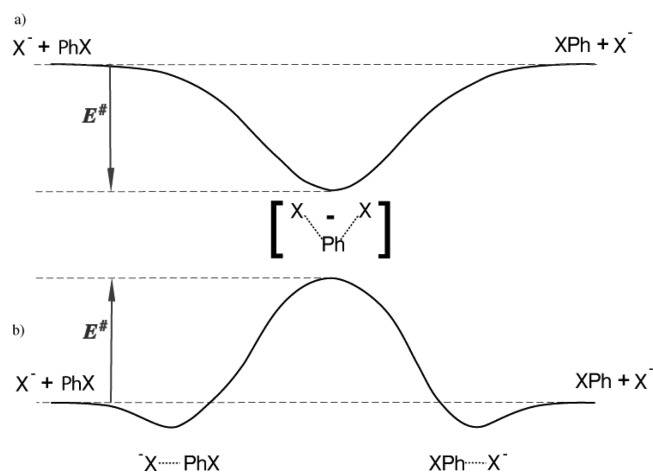(59) Uggerud, E. *J. Chem. Soc., Perkin Trans. 2* **1999**.

FIGURE 1. Potential energy curves for the substitution reactions. The upper curve (a) represents the situation where the Meisenheimer adduct is a minimum energy structure, while the lower curve is typical for a situation where the similar central symmetric is a transition structure (saddle point of the potential energy surface).

for which the critical energy is negative, i.e., the Meisenheimer adduct is stable. On the way from infinitely separated reactants, X^- + PhX, to infinitely separated products, PhX + X^-, there is essentially only one intermediate geometrical point to be considered, that is the energy minimum corresponding to the symmetrical Meisenheimer adduct. The alternative energy diagram, encountered for less reactive combinations of substrates and nucleophiles, is illustrated in Figure 1b. This is an example of a double-well potential energy function. Besides the symmetrical structure, $[X\cdots Ph\cdots X]^-$, which in this case is a transition structure and not a potential energy minimum, there are minima corresponding to the ion/molecule complexes $[XPh\cdots X]^-$ and $[X\cdots PhX]^-$. The energy difference between the Meisenheimer adducts (irrespective of whether it is a minimum or not) and the separated reactants X^- + PhX gives the critical energy ($E^{\ddagger}$) in both situations (a) and (b). Note that $E^{\ddagger}$ has a negative value when the Meisenheimer adduct is a minimum. In the absence of a central energy barrier (b) collapses into (a). We need to point out that in some cases there may exist additional electrostatically bonded complexes that may or may not be lower in energy than the Meisenheimer adduct, but they are remote from the transition structure on the potential energy surface.[22] This was, for example, shown to be the case for F^- + PhF, for which there is a minimum for $F^-\cdots$PhF with the fluoride ion attached to the hydrogen in the *para*-position. Such energetically stable complexes may represent transient species along the actual reaction path and may therefore to some extent affect the overall reaction kinetics, but for the present principal discussion about the factors affecting covalent bond breaking and bond formation we will not dwell on these complexes since they are not energy limiting.

We will now present the results of our calculations. For each reaction considered, we carried out full geometry optimizations and calculated the energies of the separated reactants and the Meisenheimer structure. In addition to this, we performed EDA calculations of a selected subset of the reactions. The characteristics of the EDA profiles and the nature of the Meisenheimer structure (TS or minimum)

make it possible to categorize a reaction to either type (a) or (b) of Figure 1.

Energetics and Role of Substrate and Nucleophile. Starting with the monosubstituted benzenes, we observe (Table 1) that the OPBE critical energies computed for the halides agree quantitatively very well with the MP2 and B3LYP critical energies computed by Glukhovstev,[22] and with their observation that the identity reaction with X = F is of type (a) while for X = Cl and Br they are of type (b). The fluoride reaction has a considerable negative critical energy, while chloride and bromide have equally significant positive values, with the latter figures being close to each other. We note a similar behavior for the group 16 congeners, in the sense that X = OH gives a stable Meisenheimer adduct, while X = SH and SeH give transition structures. In parallel with this, the critical energy for the reaction with hydroxide ion is substantially lower than for those of the hydrogen sulfide and hydrogen selenide ions. The same periodic tendency also applies to group 15 species $X^- = NH_2^-$, PH_2^-, and AsH_2^-. Furthermore, we see that the $E^{\ddagger}$ values for X = NH_2, OH, and F are not very different from each other, all being in the range -53 to -41 kJ mol^{-1}, but with a slight lean toward less stability in going from left to right in the periodic table.

Table 1 also includes a number of identity reactions involving polysubstituted benzenes with X = F, OH, NH_2, Cl, and SH. From Table 1 we observe that substitution with electron-withdrawing substituents decreases the critical energy by stabilizing the Meisenheimer adduct compared to the reactants, in full agreement with expectations. This substituent effect can be analyzed in several ways, including traditional Hammett plots. In order to provide a more self-consistent approach linking to a physical observable rather than a set of tabulated empirical parameters or atomic population charges, we decided to use the calculated C(1s) orbital energy of the always well-localized 1s orbital of the central carbon atom of the substrate molecule as the variable to which we relate the observed barriers. Core ionization energy (IE), as determined by X-ray photoelectron spectroscopy experiments, is known to be a useful descriptor of the local electronic environment.[60] For example, within a given class of compounds (e.g., alcohols), the proton affinity is linearly correlated to IE(1s).[61,62] Strictly speaking, putting IE(1s) = $-E$(1s) (Koopmans' theorem) is a rather coarse approximation in this case, since among other factors, the electron density relaxes during a core ionization event. However, the purpose of our analysis is not to provide accurate estimates for core ionization energies but to introduce a computationally easily obtainable descriptor with a clear physical relevance related to the Lewis acidity of the reactive carbon of the substrate molecule. The final result of the analysis is displayed in Figure 2. Interestingly, besides documenting the fact that the Meisenheimer adduct becomes more stable by the presence of electron-withdrawing groups, the plot has other interesting features. The most evident is that for a given nucleophile the correlation is linear. In addition, we notice the close parallelism between the five lines determined by the best linear fit to the data set for

(60) Saethre, L. J.; Thomas, T. D. *J. Org. Chem.* **1991**, *56*, 3935.
(61) Martin, R. L.; Shirley, D. A. *J. Am. Chem. Soc.* **1974**, *96*, 5299.
(62) Davis, D. W.; Rabalais, J. W. *J. Am. Chem. Soc.* **1974**, *96*, 5305.

TABLE 1.   Energy and Data Obtained with OPBE/6-311++G(d,p)

X	R_1	$R_2 = R_3$	Meisenheimer	TS ($\nu^{\ddagger}$, cm^{-1}) ^{a}	$E^{\ddagger b}$(kJ/mol)	E(1s-C) ^{c}(hartees)
F	NH$_2$	H	YES		−16.2	−9.837
F	OH	H	YES		−24.2	−9.846
F	Me	H	YES		−34.7	−9.847
F	H	H	YES		−40.6	−9.853
F	C≡CH	H	YES		−90.9	−9.862
F	CHO	H	YES		−131.9	−9.877
F	CN	H	YES		−130.8	−9.882
F	NO$_2$	H	YES		−153.2	−9.886
Cl	H	H		YES (i·287)	+99.1	−9.832
Cl	F	H		YES (i·299)	+93.8	−9.837
Cl	NO$_2$	H		YES (i·115)	+5.1	−9.863
Cl	NO$_2$	NO$_2$	YES		−102.7	−9.910
Br	H	H		YES (i·249)	+106.5	−9.827
OH	H	H	YES		−52.2	−9.821
OH/F	NO$_2$	H	YES		−115.2	−9.856
OH	NO$_2$	H	YES		−176.3	−9.856
OH	NO$_2$	NO$_2$	YES		−303.0	−9.915
SH	H	H		YES (i·242)	+76.4	−9.806
SH	NO$_2$	H	YES		−34.6	−9.838
SH	OH	H		YES (i·291)	+87.6	−9.800
SH	NO$_2$	NO$_2$	YES		−152.2	−9.892
SeH	H	H		YES (i 234)	+83.0	−9.804
NH$_2$	H	H	YES		−53.1	−9.788
NH$_2$	NH$_2$	H	YES		−33.8	−9.776
NH$_2$	NO$_2$	H	YES		−182.8	−9.824
NH$_2$	NO$_2$	NO$_2$	YES		−295.3	−9.890
PH$_2$	H	H		YES (i·112)	+38.7	−9.778
AsH$_2$	H	H		YES (i·174)	+54.0	−9.778

^{a}Vibrational frequency corresponding to the reaction coordinate. ^{b}Critical energy, i.e., energy difference between central complex (stable Meisenheimer adduct or TS) and reactants (zero point vibrational energies included). ^{c}Core electron orbital energy of the reaction central carbon atom of the reactant molecule.
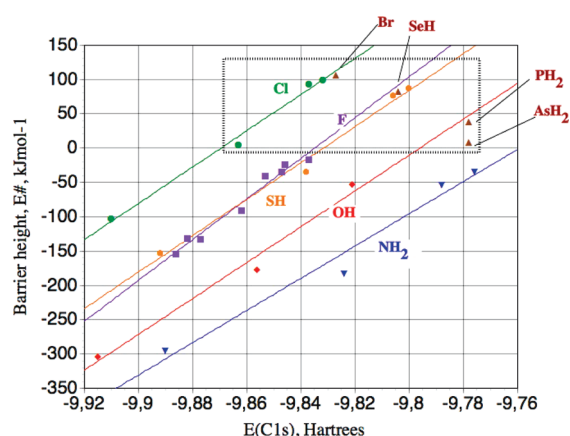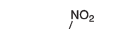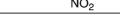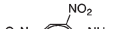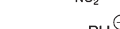

FIGURE 2. Calculated barrier height for aromatic substitution versus the 1s orbital energy associated with the *ipso* carbon of the substrate (R$_1$,R$_2$,R$_3$)-PhX. The energy data have been taken from Table 1. Each line corresponds to a given nucleophile X$^-$ for a range of ring substituents R$_1$, R$_2$, and R$_3$ and is obtained by a least-squares linear fit to the data points. The hatched box contains all data points for which the symmetrical structure is a TS.

each of the five nucleophiles/nucleofuges considered. This demonstrates two points, namely that E(1s) of the substrate's *ipso* carbon is an excellent descriptor of the electronic effect on $E^{\ddagger}$ and that each of the X series have nearly identical susceptibilities to the R$_1$, R$_2$, R$_3$ substituent effect.

General Geometrical Factors. Table 2 shows the essential geometric information. We define the bond elongation factor $\varepsilon = (r_M - r_S)/r_S$, where r_S is the equilibrium C–X bond distance in the substrate molecule and r_M is the same in the Meisenheimer adduct/TS. For the monosubstituted series X = NH$_2$, OH, and F we observe relatively little variation in this quantity, with values of 0.086, 0.081, and 0.096, respectively, a variation that is of the same order as the variation in $E^{\ddagger}$. Stepping down from period 2 to period 3 of the periodic table, we observe a considerable increase in ε, being 0.137 for X = SH and 0.177 for Cl. For X = Br it is 0.195.

Turning our attention toward the polysubstituted benzenes, considering each nucleophile separately, we note that the C–X bond distances of the Meisenheimer adduct vary to a considerably larger degree than for the substrate. For example, for X = F the difference between the shortest (-*p*-NO$_2$) and the longest (-*p*-NH$_2$) bond variation is 0.012 Å in the substrate, while the corresponding figure is 0.040 Å for the Meisenheimer adduct. We will not speculate on the exact relationship between the variation in bond lengths and the relative weight of the two structures in determining the variation in the critical energy, except to state that it is not obvious that this shows that one is more important than the other. Inspection of the variation of the bond elongation factor is more rewarding. Within each series of nucleophiles there is a tendency that ε decreases upon substitution by electronegative substituents, matching the drop in $E^{\ddagger}$.

TABLE 2. Key Geometrical Data Obtained with OPBE/6-311++G(d,p)

Substrate	r (C-X) / Å	Complex	r (C-X) / Å	X···C···X / degrees
H_2N—C$_6$H$_4$—F	1.353	H_2N—C$_6$H$_4$(F)(F)⁻	1.480	96.1
HO—C$_6$H$_4$—F	1.351	HO—C$_6$H$_4$(F)(F)⁻	1.478	95.8
Me—C$_6$H$_4$—F	1.350	Me—C$_6$H$_4$(F)(F)⁻	1.477	96.1
H—C$_6$H$_4$—F	1.349	H—C$_6$H$_4$(F)(F)⁻	1.479	96.1
HC≡C—C$_6$H$_4$—F	1.346	HC≡C—C$_6$H$_4$(F)(F)⁻	1.458	97.7
OHC—C$_6$H$_4$—F	1.342	OHC—C$_6$H$_4$(F)(F)⁻	1.445	98.8
NC—C$_6$H$_4$—F	1.342	NC—C$_6$H$_4$(F)(F)⁻	1.451	98.3
O_2N—C$_6$H$_4$—F	1.341	O_2N—C$_6$H$_4$(F)(F)⁻	1.440	99.3
H—C$_6$H$_4$—Cl	1.735	H—C$_6$H$_4$(Cl)(Cl)⁻	2.042	95.3
F—C$_6$H$_4$—Cl	1.734	F—C$_6$H$_4$(Cl)(Cl)⁻	2.050	95.0
O_2N—C$_6$H$_4$—Cl	1.726	O_2N—C$_6$H$_4$(Cl)(Cl)⁻	1.938	99.4
O_2N,NO_2—C$_6$H$_2$—Cl (NO_2)	1.704	O_2N,NO_2—C$_6$H$_2$(Cl)(Cl)(NO_2)⁻	1.849	107.4
H—C$_6$H$_4$—Br	1.892	H—C$_6$H$_4$(Br)(Br)⁻	2.260	95.3
H—C$_6$H$_4$—OH	1.363	H—C$_6$H$_4$(OH)(OH)⁻	1.473	97.8
O_2N—C$_6$H$_4$—OH	1.353	O_2N—C$_6$H$_4$(F)(OH)⁻	C-F:1.523, C-0:1.413	101.5
O_2N—C$_6$H$_4$—OH	1.353	O_2N—C$_6$H$_4$(OH)(OH)⁻	1.482, 1.433	101.6
O_2N,NO_2—C$_6$H$_2$—OH (NO_2)	1.314	O_2N,NO_2—C$_6$H$_2$(OH)(OH)(NO_2)⁻	1.448, 1.384	107.1
H—C$_6$H$_4$—SH	1.769	H—C$_6$H$_4$(SH)(SH)⁻	2.000, 2.023	96.3
O_2N—C$_6$H$_4$—SH	1.758	O_2N—C$_6$H$_4$(SH)(SH)⁻	1.959, 1.896	111.2
HO—C$_6$H$_4$—SH	1.772	HO—C$_6$H$_4$(SH)(SH)⁻	2.038	93.2
O_2N,NO_2—C$_6$H$_2$—SH (NO_2)	1.742	O_2N,NO_2—C$_6$H$_2$(SH)(SH)(NO_2)⁻	1.865, 1.893	106.5
H—C$_6$H$_4$—SeH	1.911	H—C$_6$H$_4$(SeH)(SeH)⁻	2.196, 2.205	95.6
H—C$_6$H$_4$—NH_2	1.392	H—C$_6$H$_4$(NH_2)(NH_2)⁻	1.512	102.9
H_2N—C$_6$H$_4$—NH_2	1.403	H_2N—C$_6$H$_4$(NH_2)(NH_2)⁻	1.512	102.8
O_2N—C$_6$H$_4$—NH_2	1.374	O_2N—C$_6$H$_4$(NH_2)(NH_2)⁻	1.495	104.5
O_2N,NO_2—C$_6$H$_2$—NH_2 (NO_2)	1.332	O_2N,NO_2—C$_6$H$_2$(NH_2)(NH_2)(NO_2)⁻	1.468, 1.474	107.5
H—C$_6$H$_4$—PH_2	1.843	H—C$_6$H$_4$(PH_2)(PH_2)⁻	1.978	99.6
H—C$_6$H$_4$—AsH_2	1.965	H—C$_6$H$_4$(AsH_2)(AsH_2)⁻	2.146	98.3

From Table 2 we also note interesting trends in the variation of the X···C···X bond angle of the Meisenheimer adduct with respect to variation in nucleophile and substrate substitution. The general trend seems to be that the bond angle increases with relative stabilization of the Meisenheimer adduct, both with regard to nucleophile, both from right to left in a row, and with regard to electron accepting substitution. It thus seems that the most stabilized Meisenheimer adducts allow for higher sp^3 character, giving more obtuse X···C···X angles that are closer to the ideal tetrahedral arrangement.

Aromatic Character of the Meisenheimer Adduct. As stated above, formation of Meisenheimer adducts may at first sight appear counterintuitive since the benzene π-electron system is broken. Before proceeding, it became necessary to gain more insight into the relationship between the energy requirements for adduct formation and changes in the geometric and electronic structure of the aromatic ring. We will discuss two typical cases, the PhOH + OH⁻ reaction (which leads to the minimum energy Meisenheimer adduct Ph(OH)$_2$⁻) and the PhSH + SH⁻ reaction (which leads the transition structure Ph(SH)$_2$⁻, see Table 1).

The benzene-like structure, often referred to by the term aromaticity, has manifold definitions. One very useful and easily obtainable criterion is the HOMA value,[44,45] which reflects the deviation from the ideal geometry in which all C−C bonds of the ring are of equal length. As readily seen in Figure 3, the change in the C−C bond lengths is clearly more pronounced in going from PhOH to Ph(OH)$_2$⁻ than from PhSH to Ph(SH)$_2$⁻. While PhOH and PhSH present the same HOMA value (HOMA = 0.98) confirming their aromatic character, Ph(OH)$_2$⁻ exhibits a considerably lower HOMA value (HOMA = 0.40) compared to Ph(SH)$_2$⁻ (HOMA = 0.75). In other words, applying this simple geometric criterion, the more stable Meisenheimer adduct Ph(OH)$_2$⁻ preserves significantly less aromatic character than the less stable Ph(SH)$_2$⁻ transition structure. This is a general periodic trend. The reaction systems belonging to period 2 (X⁻ = NH$_2$⁻, OH⁻, and F⁻) form Meisenheimer adducts with low HOMA values, while the reaction systems having nucleophiles/nucleofuges from period 3 and 4 do not form stable Meisenheimer adducts. The corresponding TS structures all have comparably higher HOMA values.

In principle, bond length equalization in aromatic compounds may in some cases primarily result from σ interactions and less from π bonding. The latter may even become stronger in bond alternating geometries.[63−66] Therefore, the use of geometry-based aromaticity indices (like HOMA) has been criticized. Whether this criticism also applies to the situations described here is, however, questionable. Irrespective of this, we wanted also to use an electronic structure criterion to clarify the situation and decided to study magnetic induction. For this purpose, the visual representations of induced current densities as implemented in the AICD approach are useful[53,54] Figure 3 shows that, while the induced current is strong and diatropic in PhOH and PhSH (which is a typical aromatic characteristic), the current is

(63) Shaik, S. S.; Bar, R. *Nouv. J. Chim.* **1984**, *8*, 411.
(64) Shaik, S. S.; Shurki, A.; Danovich, D.; Hiberty, P. C. *Chem. Rev.* **2001**, *101*, 1501.
(65) Fernández, I.; Frenking, G. *Faraday Discuss.* **2007**, *135*, 403.
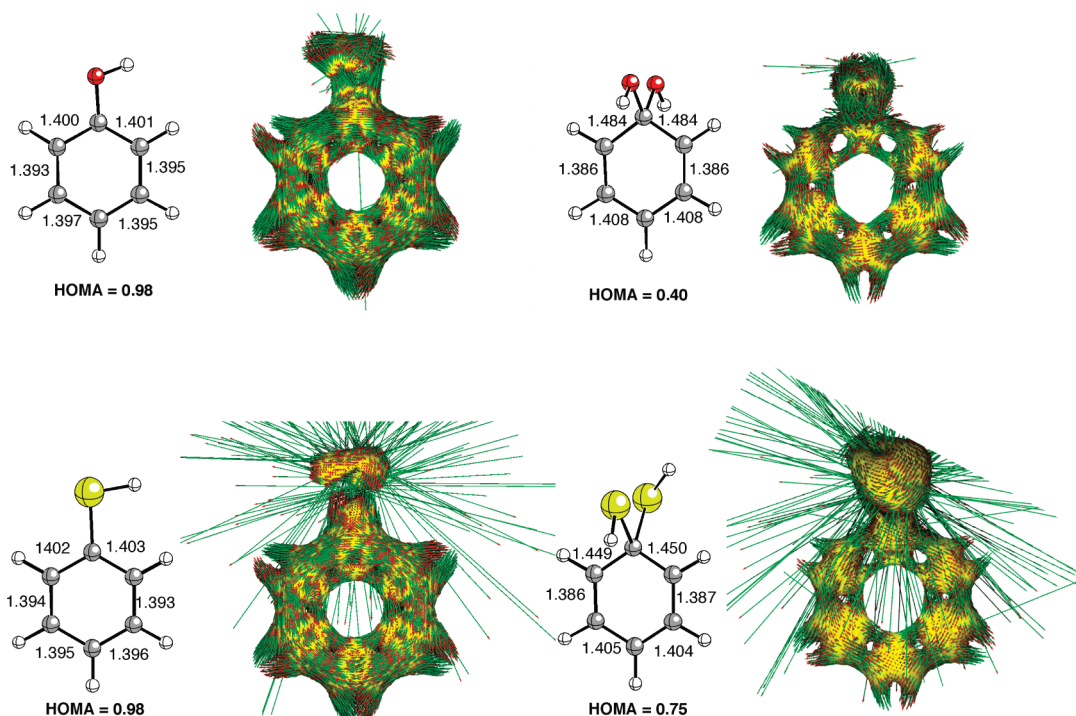(66) Pierrefixe, S. C. A. H.; Bickelhaupt, F. M. *Chem.—Eur. J.* **2007**, *13*.

FIGURE 3. Ball-and-stick representation of PhOH, Ph(OH)$_2^-$, PhSH, and Ph(SH)$_2^-$ together with their corresponding HOMA values and AICD plots (isosurface level of 0.05); see text. Bond lengths are given in Å. The data have been obtained with OPBE/6-311++G(d,p).

clearly more disrupted in Ph(OH)$_2^-$ than in Ph(SH)$_2^-$. This is an indication of higher aromatic character in the latter molecule. These graphical representations therefore nicely agree with the conclusions drawn using the HOMA values.

Energy Decomposition Analysis (EDA). In full accordance with our study of the S$_N$2 reaction, we apply a scheme for EDA, separating the supermolecule into two parts, Ph$^+$ + [X···X]$^{2-}$, using the situation with infinite separation between the two X$^-$ units as the common point of reference for all energy calculations. In this way, the binding situation at any point along the entire reaction path, including reactant minima, transition structures, and other intermediate structures of interest, can be analyzed in a direct manner as a function of the reaction coordinate r(C···X) (the distance between the reactive carbon center and the approaching nucleophile). The two points of particular interest are as follows: (i) PhX + X$^-$ having one of the r(C···X) = ∞, which represents the formation of PhX from the components Ph$^+$ and X$^-$ and corresponds to the reactant structure, and (ii) the Meisenheimer structure in which both C–X distances have the same value. In addition, the presence of other stationary points along the reaction coordinate can be subject to examination in this manner. In the following discussion, we will concentrate our attention to the end points of the reaction, namely (i) and (ii), since only these structures determine the critical energy (the energy difference).

In forming aniline, phenol, and fluorobenzene from the ionic building blocks Ph$^+$ + X$^-$ (X$^-$ = NH$_2^-$, OH$^-$, and F$^-$, respectively; see Figure 4 and Table 3) we note that the energies of formation (phenyl cation affinity) are of the same order and follow the sequence NH$_2^-$ > OH$^-$ > F$^-$. This trend in phenyl cation affinities parallels the trend in the proton affinities of the X$^-$ species. This is expected since there exists an analogous and well-established linear relationship

between various alkyl cation affinities and proton affinity, demonstrating the close relationship between carbon and hydrogen basicity in the gas phase.[67] Following the approach of the nucleophile to the substrate it is fascinating to register the development in the various energy terms on the route from reactants PhX + X$^-$ to Meisenheimer structure for these three reactions (Figure 4a–c). A common feature is the continuous increase in the attractive forces (orbital and electrostatic interaction) with a concurrent build-up of Pauli repulsion, neatly illustrating how adduct formation results from balancing attractive and repulsive interactions. The energy curves of Figure 4a–c show remarkable similarities. Although each energy component in absolute terms always is largest for amide and smallest for fluoride, the similar shapes make the relative contributions to the reactant and the Meisenheimer structures almost the same. In terms of the Lewis acid/base hypothesis implicit in our analysis,[68] the higher Lewis basicity of amide relative to hydroxide and fluoride is neatly compensated by the lower Lewis acidity (in terms of C(1s) energies, Figure 2) of the *ipso* carbon of aniline compared to phenol and fluoro. Consequently, the $E^\ddagger$ values of the reactions of the triade of this period are identical within a few kcal/mol. From this analysis, we note a fundamental difference between S$_N$Ar and S$_N$2 intrinsic nucleophilicity. For the S$_N$2 reaction the periodic trend is the opposite and is significantly stronger, with $E^\ddagger$ values of −6, 59, and 118 kJ mol^{-1} for X$^-$ = NH$_2^-$, OH$^-$, F$^-$, respectively,[26] with all three reactions having the type b potential energy profile of Figure 1.

Returning to S$_N$Ar, in going from F$^-$ to Cl$^-$ (Figure 4c,d), we see a different picture. The value for each energy term

(67) Uggerud, E. *Eur. Mass Spectrom* **2000**, *6*, 131.
(68) Roland, L.; Robert, L.; Herbert, M. *Angew. Chem., Int. Ed.* **2002**, *41*, 91.
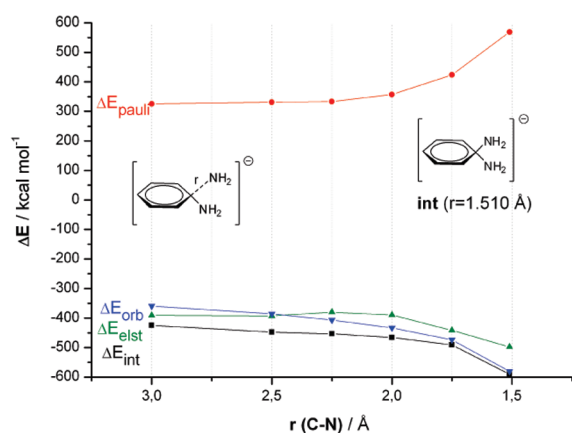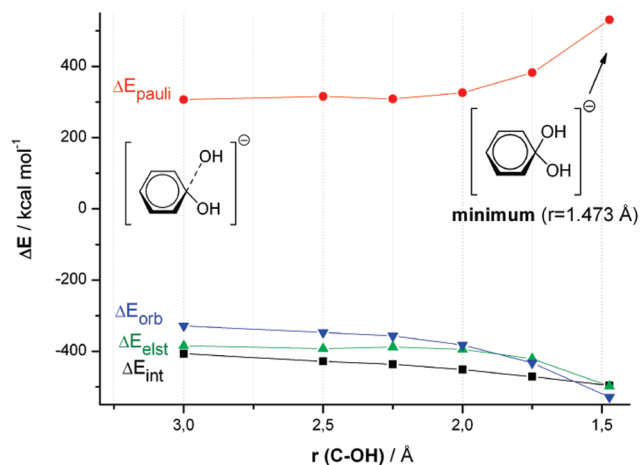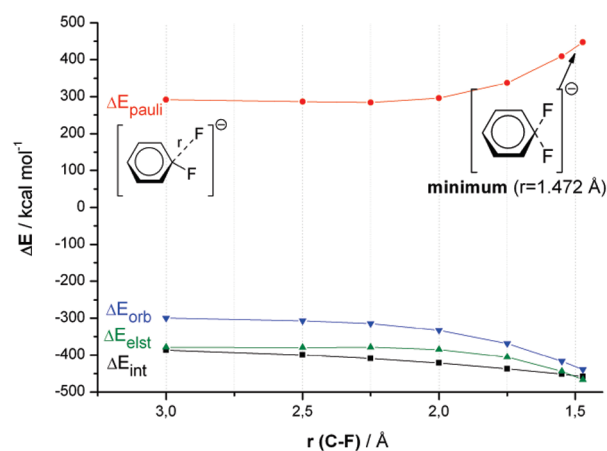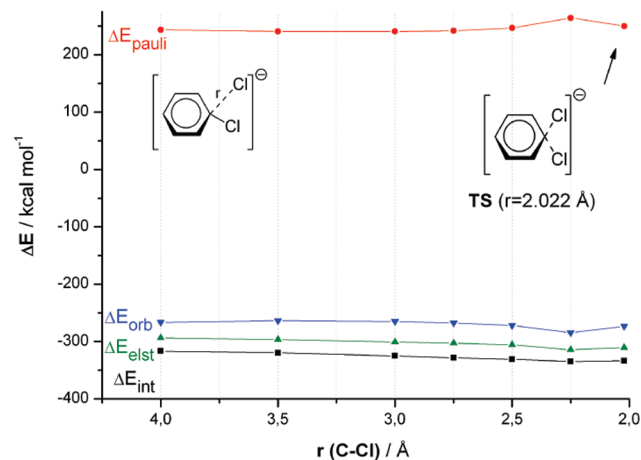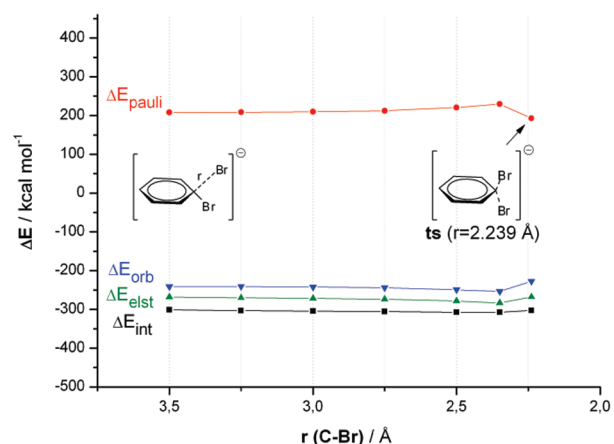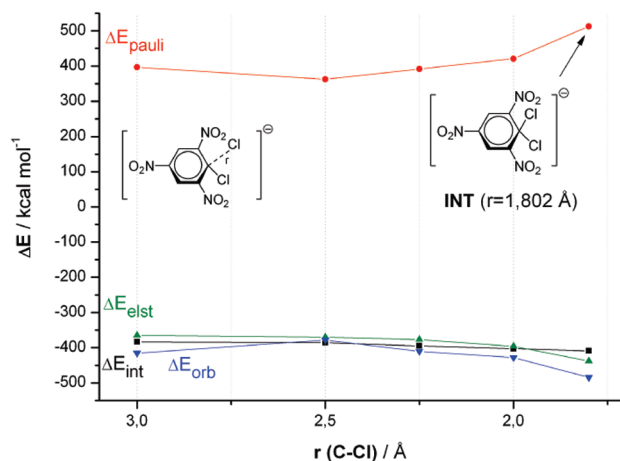
FIGURE 4. EDA plots for selected S_NAr processes.

(Pauli, orbital, electrostatic) is significantly smaller in absolute terms, and the curve shapes are also different. In the case

of Cl⁻, each term does not change much along the reaction coordinate from reactants to Meisenheimer transition structure,

TABLE 3. Change in the Energy Terms of the EDA for the Systems [PhX···X]⁻ and the Tetracoordinated Systems [X···Ph···X]⁻ where Both C−X Distances Are Identical[a]

PhF/F⁻						
$r(C\cdots F)$	3.0	2.5	2.25	2.0	1.75	1.55	1.472 (min)
$\Delta\Delta E_{int}$	0.0	−13.0	−22.5	−35.0	−50.5	−64.8	−71.4
$\Delta\Delta E_{Pauli}$	0.0	−5.3	−7.6	4.1	45.1	117.3	155.5
$\Delta\Delta E_{elstat}$	0.0	−0.5	−0.1	−6.1	−26.6	−65.2	−87.7
$\Delta\Delta E_{Orb}$	0.0	−7.2	−14.8	−33.0	−69.0	−117.0	−139.3
$\Delta\Delta E_{prep}$	0.0	11.5	19.6	29.9	42.3	53.9	60.0
$\Delta\Delta E$	0.0	−1.5	−2.9	−5.1	−8.2	−10.9	−11.4

PhCl/Cl⁻						
$r(C\cdots Cl)$	4.0	3.5	3.0	2.75	2.5	2.25	2.022 (ts)
$\Delta\Delta E_{int}$	0.0	−2.8	−8.3	−11.7	−14.3	−18.0	−17.0
$\Delta\Delta E_{Pauli}$	0.0	−2.9	−2.8	−1.6	3.2	20.8	6.6
$\Delta\Delta E_{elstat}$	0.0	−3.1	−7.2	−9.3	−12.2	−20.8	−16.9
$\Delta\Delta E_{Orb}$	0.0	3.1	1.7	−0.8	−5.3	−18.0	−6.7
$\Delta\Delta E_{prep}$	0.0	4.2	13.4	19.8	26.1	34.4	37.9
$\Delta\Delta E$	0.0	1.4	5.1	8.1	11.8	16.4	20.9

PhBr/Br⁻						
$r(C\cdots Br)$	3.5	3.25	3.0	2.75	2.5	2.35	2.239 (ts)
$\Delta\Delta E_{int}$	0.0	−1.8	−3.2	−4.5	−6.0	−6.1	−1.4
$\Delta\Delta E_{Pauli}$	0.0	0.5	1.6	4.2	12.7	21.8	−15.0
$\Delta\Delta E_{elstat}$	0.0	−1.8	−3.6	−5.6	−10.2	−15.2	0.3
$\Delta\Delta E_{Orb}$	0.0	−0.3	−1.1	−2.9	−8.3	−12.5	−13.5
$\Delta\Delta E_{prep}$	0.0	3.9	8.1	13.3	19.6	23.1	20.8
$\Delta\Delta E$	0.0	2.1	4.9	8.8	13.6	17.0	19.4

2,4,6-NO₂-PhCl/Cl⁻						
$r(C\cdots Cl)$	3.0	2.5	2.25	2.0	1.802 (min)	1.908 (ts)
$\Delta\Delta E_{int}$	0.0	−2.2	−11.5	−19.6	−25.8	−6.2
$\Delta\Delta E_{Pauli}$	0.0	−34.7	−5.2	23.9	116.0	−90.2
$\Delta\Delta E_{elstat}$	0.0	−5.1	−11.6	−30.9	−73.3	6.8
$\Delta\Delta E_{Orb}$	0.0	37.6	5.3	−12.6	−68.6	77.1
$\Delta\Delta E_{prep}$	0.0	−0.6	6.7	11.0	15.4	15.9
$\Delta\Delta E$	0.0	−2.8	−4.8	−8.6	−10.4	9.1

PhOH/OH⁻						
$r(C\cdots OH)$	3.0	2.5	2.25	2.0	1.75	1.473 (min)
$\Delta\Delta E_{int}$	0.0	−21.4	−29.4	−44.7	−64.4	−89.1
$\Delta\Delta E_{Pauli}$	0.0	9.0	1.8	19.1	75.6	224.4
$\Delta\Delta E_{elstat}$	0.0	−8.1	−3.4	−10.3	−36.4	−113.5
$\Delta\Delta E_{Orb}$	0.0	−18.3	−27.8	−53.5	−103.6	−200.0
$\Delta\Delta E_{prep}$	0.0	19.5	24.9	35.8	48.7	66.7
$\Delta\Delta E$	0.0	−1.9	−4.5	−8.9	−15.7	−22.4

PhNH₂/NH₂⁻						
$r(C\cdots NH_2)$	3.0	2.5	2.25	2.0	1.75	1.510 (min)
$\Delta\Delta E_{int}$	0.0	−22.8	−28.5	−41.0	−66.2	−165.7
$\Delta\Delta E_{Pauli}$	0.0	5.7	8.0	31.8	98.7	243.7
$\Delta\Delta E_{elstat}$	0.0	−2.0	10.9	1.3	−50.7	−107.1
$\Delta\Delta E_{Orb}$	0.0	−26.6	−47.3	−74.1	−114.2	−221.3
$\Delta\Delta E_{prep}$	0.0	20.4	21.3	32.1	51.7	145.6
$\Delta\Delta E$	0.0	−2.4	−7.2	−8.9	−14.5	−20.1

[a]Energy values in kcal/mol, distances in Å. All data have been computed at the OPBE/TZ2P level.

but we note that the Pauli term increases slightly more than the ΔE_{int} term decreases. This together with a less favorable contribution from ΔE_{prep} (Table 3) results in the significantly positive $E^{\ddagger}$ value of +83 kJ mol⁻¹. The continuous increase in ΔE_{Pauli} up to $r = 2.25$ Å and a slight decrease further to the symmetrical Meisenheimer transition structure is consistent with the topography of this part of the potential energy surface, where the Meisenheimer structure gives a maximum along the $r(C\cdots X)$ reaction coordinate. The same type of behavior is essentially observed for Br⁻ as for Cl⁻ (Figure 4 e). Comparison between panels d and f of Figure 4 reveals the strong stabilizing effect of electron-withdrawing substituents. The reaction between chloride ion and 2,4,6-trinitrophenyl chloride is very different from that between chloride

and unsubstituted phenyl chloride. In the former case, the electronic effect is stabilizing by making the Meisenheimer structure a potential energy minimum rather than a maximum along the $r(C \cdots X)$ reaction coordinate. As a result, the EDA profile has more in common with the fluoride of panel c than the chloride of panel d. We may conclude this section by stating that EDA provides a useful and consistent illustration of the periodic trends in the development of the various contributions to the total binding energy along the reaction path, both with regard to the great similarities observed within the nucleophiles belonging to the same period of the periodic table as well as the considerable change observed moving down from period 2 to 3 and far less from 3 to 4.

Final Discussion. The findings presented above provide the basis for rationalizing the periodic trends. We will now primarily consider the unsubstituted PhX systems. As already noted, the very similar stabilities of the three Meisenheimer adducts of period 2 are due to a compromise between the relative Lewis basicity of the nucleophile X^- and the relative Lewis acidity of the reactive carbon atom of PhX, the relative basicity being highest for NH_2^- and the acidity being highest for PhF. Parallel trade-offs can also be found within the period 3 and period 4 triads. However, the change in the value of $E^{\ddagger}$ in stepping down from period 2 to period 3 is yet to be explained. Again, we need to consider relative Lewis acidities and basicities. There is a marked drop in the Lewis (and Brønsted) basicity of the nucleophile X^- in going down in one group from row 2 to row 3. At the same time, there is a drop in carbon acidity (Table 1, Figure 2). This leads to significantly weaker binding, with a resulting unstable Meisenheimer adduct. This is of course related to the fact that forming molecular orbitals from atomic orbitals both having principal numbers n of 2 is more rewarding than combining one with $n = 2$ with one with $n = 3$. The increases in $E^{\ddagger}$ in stepping down from period 3 to 4 are, however, less pronounced. Carbon acidity is approximately conserved, while Lewis basicity only decreases slightly.

At this point, we are able to understand the "counterintuitive" aromaticity breaking behavior. Ideally, formation of a new C−X bond leading to the Meisenheimer adduct will change the hybridization of the central carbon from sp^2 to sp^3 ending up with a perfect tetrahedral bonding arrangement around this atom. In association with this there will be a considerable decrease in potential energy resulting from the newly formed bond. On the other hand, the tetrahedral geometric arrangement has a high price by breaking the aromatic character of the ring. Upon forming a perfectly tetrahedral Meisenheimer adduct, the molecular system needs to sacrifice the aromatic delocalization energy as well as one π-bond, at least in principle. The geometry data of Table 2 and Figure 3 reveal a slightly more composite picture since none of the Meisenheimer adducts are able to obtain the perfect structure described here. For example, the $X \cdots C \cdots X$ bond angle is always considerably less than

109.5°, and the two C−C bonds to the central carbon are always shorter than the typical single bond. Therefore, each system adopts to the general requirement of balancing the loss of aromaticity by the formation of a new C−X bond. This is again evident from Figure 3. For OH^- with the ability of forming a strong dative bond to the carbon of the substrate molecule phenol, the ring offers more of its aromatic character in forming the Meisenheimer adduct compared to SH^-, which forms a considerably weaker bond to thiophenol.

Conclusions

For the identity substitution reaction $X^- + PhX \rightarrow X^- + PhX$ (Ph = phenyl) all period 2 nucleophiles are approximately equally reactive but significantly more reactive than their period 3 and 4 analogues, $NH_2^- \approx OH^- \approx F^- \gg PH_2^- \approx SH^- \approx Cl^- > AsH_2^- \approx SeH^- \approx Br^-$, which defines the periodic trend in relative intrinsic nucleophilicities. This trend is clearly different from the corresponding trends in basicity. However, for any actual substitution reaction where the nucleophile and leaving group are different, i.e., $Y^- + PhX \rightarrow X^- + PhY$, the exothermicity of the reaction will also come into play: the more exothermic the reaction is, the higher is the contribution from the thermochemical driving force relative to that of the intrinsic nucleophilicities. The reaction exothermicity correlates with the difference in Brønsted basicity between nucleophile and leaving group.

This study also demonstrates that the intrinsic nucleophilicity in S_NAr reactions is very different from the nucleophilicity in S_N2 processes. In other words, there seems to be no universal nucleophilicity scale valid for all types of nucleophilic substitution reactions. Only in the extreme cases of very exothermic reactions will the two types of nucleophilicity merge due to the dominating thermochemical driving force term in the Marcus expression.

Supporting Information Available: One table of results from the energy decomposition analysis and one table containing Cartesian coordinates and energies of all species described. This material is available free of charge via the Internet at http://pubs.acs.org.